Genes & Nutrition

RESEARCH Open Access

Sodium butyrate suppresses endometrial cancer cell growth by inhibiting thymidylate synthase and reprogramming pyrimidine metabolism

Nayeon Kim[1], Sooyeon Park[1] and Changwon Yang[1*]

Abstract

Endometrial cancer (EC) is the most common gynecologic malignancy, yet effective therapies for advanced and recurrent disease remain limited. Sodium butyrate (NaB), a gut microbiota-derived short-chain fatty acid (SCFA) with known anticancer activity, remains poorly understood in EC. In this study, we investigated the anticancer effects of NaB in two EC cell lines, HEC1A and AN3CA. NaB dose-dependently inhibited cell viability, colony formation, and migration in both cell lines, with HEC1A cells exhibiting greater sensitivity. NaB differentially modulated epithelial-mesenchymal transition (EMT)-related markers between the two cell lines. NaB markedly induced apoptosis in HEC1A cells, whereas AN3CA cells showed resistance to apoptotic cell death, despite mitochondrial membrane depolarization occurring in both cell lines. Cell cycle analysis revealed subG1-accumulation in HEC1A cells and G1 phase arrest in AN3CA cells. Notably, NaB potently suppressed thymidylate synthase (TS) at both mRNA and protein levels in both cell lines, representing the first demonstration of TS suppression by NaB in EC. NaB also broadly reprogrammed pyrimidine metabolism by downregulating de novo synthesis enzymes while upregulating salvage pathway components. Taken together, these findings suggest that TS suppression and pyrimidine metabolic reprogramming are important components of the in vitro response of EC cells to NaB. These results provide mechanistic insight into the metabolic effects of NaB in EC and support further investigation of this pathway in pharmacologically relevant and locally applicable therapeutic contexts.

Keywords Endometrial cancer, Sodium butyrate, Thymidylate synthase, Pyrimidine metabolism, Cell cycle

*Correspondence:
Changwon Yang
cyang@ewha.ac.kr
[1]Department of Science Education, College of Education, Ewha Womans University, Seoul 03760, Republic of Korea

© The Author(s) 2026. **Open Access** This article is licensed under a Creative Commons Attribution-NonCommercial-NoDerivatives 4.0 International License, which permits any non-commercial use, sharing, distribution and reproduction in any medium or format, as long as you give appropriate credit to the original author(s) and the source, provide a link to the Creative Commons licence, and indicate if you modified the licensed material. You do not have permission under this licence to share adapted material derived from this article or parts of it. The images or other third party material in this article are included in the article's Creative Commons licence, unless indicated otherwise in a credit line to the material. If material is not included in the article's Creative Commons licence and your intended use is not permitted by statutory regulation or exceeds the permitted use, you will need to obtain permission directly from the copyright holder. To view a copy of this licence, visit http://creativecommons.org/licenses/by-nc-nd/4.0/.

Introduction

Endometrial cancer (EC) is the most common gynecologic malignancy and the sixth leading cause of cancer-related death among women worldwide [1–3]. The incidence of EC has increased across multiple countries over time, particularly in countries undergoing rapid socioeconomic change [4]. Consistent with this increasing trend, the incidence of EC is expected to more than double by 2030 [5]. Although overall survival has improved, mortality from EC continues to rise [6]. Moreover, despite advances in therapeutic strategies, there is limited evidence that current chemotherapy, hormonal therapy, and radiotherapy significantly improve survival in patients with high-risk, recurrent, or advanced EC [7, 8]. These clinical limitations highlight the need for novel therapeutic targets. Cancer cells undergo metabolic reprogramming to support growth and proliferation, which is closely linked to tumor progression and resistance to conventional therapies. Therefore, therapeutic strategies targeting EC cell metabolism represent a potential approach to overcome the limitations of current treatments for EC [9, 10].

Sodium butyrate (NaB), a representative short-chain fatty acid (SCFA), is produced through the fermentation of dietary fiber by gut microbiota and has been reported to exhibit anticancer activity across various tumor models [11]. Previous studies have shown that butyrate suppresses cancer cell proliferation, induces cell death, and regulates cell cycle progression through epigenetic regulation and the modulation of key signaling pathways [12, 13]. However, studies on these anticancer effects have predominantly focused on a limited range of tumor models, such as colorectal cancer, whereas the role of butyrate in EC remains largely unexplored. Although NaB has been reported to inhibit proliferation and induce specific forms of cell death in EC cells, comprehensive analyses of the associated metabolic alterations and cell cycle regulatory mechanisms are still limited [14, 15].

Cancer cells activate nucleic acid biosynthetic pathways to support their abnormally increased proliferative demands, and nucleotide metabolism is closely associated with cell cycle progression [16]. Consequently, reduced pyrimidine availability disrupts S-phase progression and triggers replication stress, leading to cell cycle dysregulation [17]. Because rapidly proliferating cancer cells require a continuous supply of pyrimidine nucleotides for DNA replication, disruption of pyrimidine metabolism may represent an important metabolic vulnerability in EC. In particular, thymidylate synthase (TS) is a key enzyme in de novo dTMP synthesis and plays an essential role in S phase progression and DNA replication. Therefore, dysregulation of TS may directly affect the proliferative capacity of cancer cells and contribute to replication stress. Indeed, a recent integrated metabolomic and transcriptomic analysis identified pyrimidine metabolism as a pathway significantly associated with the early diagnosis of EC based on KEGG pathway analysis, and TS was proposed as one of the major biomarkers distinguishing EC from normal endometrium [18]. In addition, epidemiologic evidence has suggested that TYMS gene polymorphisms are associated with EC risk [19], further supporting the biological and clinical relevance of pyrimidine metabolism in EC. Meanwhile, given that de novo pyrimidine synthesis is closely linked to mitochondrial function, mitochondrial membrane potential (MMP) may serve as a sensitive functional indicator of this metabolic state [20–22]. Therefore, alterations in mitochondrial function may act as an important link between disrupted pyrimidine metabolism and impaired cell cycle regulation [23]. However, it remains unclear how NaB affects pyrimidine metabolic enzymes, including TS, and their downstream effects on mitochondrial function and cell cycle regulation in EC cells [22].

Beyond these metabolic and cell cycle regulatory processes, NaB may also influence cancer cell behavior through its effects on epithelial–mesenchymal transition (EMT). EMT is a biological process closely associated with cancer cell invasion, metastasis, and therapeutic resistance. In the endometrium, the tightly regulated balance between MET and EMT is essential for normal tissue homeostasis and is closely linked to the malignant progression of EC [24, 25]. EMT is characterized by decreased E-cadherin expression and increased levels of mesenchymal markers, including vimentin and N-cadherin, which collectively promote cancer cell migration and invasion [26]. Previous studies suggest that EMT is not a simple phenotypic transition but is associated with metabolic reprogramming and changes in mitochondrial function [27, 28]. Reprogramming of metabolic pathways can contribute to the induction and maintenance of EMT. In addition, NaB has also been reported to influence EMT in various cancer types [13, 29, 30]. However, the impact of NaB on EMT-related changes, mitochondrial metabolism, and cell cycle regulation in EC has not yet been fully elucidated.

In this context, we aimed to comprehensively assess the effects of NaB on cell growth, migration, apoptosis, cell cycle progression, pyrimidine metabolism, and mitochondrial membrane potential in EC cells. Two EC cell lines with distinct biological characteristics, HEC1A and AN3CA, were selected as comparative models. These cell lines have been widely used in previous studies to assess changes in cell migration and invasiveness through EMT marker analyses and are reported to exhibit distinct differences in proliferation rates and tumor aggressiveness [31, 32]. Using these models, we sought to determine whether the anticancer effects of NaB are associated with alterations in TS expression and broader remodeling of

pyrimidine metabolism, and to examine whether these effects differ according to cellular characteristics, thereby exploring both shared and cell line-specific responses.

Materials and methods

Cell culture

The human EC cell lines HEC-1 A and AN3-CA were obtained from the American Type Culture Collection (ATCC, Manassas, VA, USA). HEC-1 A cells were cultured in McCoy's 5 A medium (Cellgro, Manassas, VA, USA) supplemented with 10% fetal bovine serum (FBS) and 1% penicillin-streptomycin (P/S). AN3-CA cells were maintained in Minimum Essential Medium (MEM) (Cellgro, Manassas, VA, USA) supplemented with 10% FBS, 1% P/S. Both cell lines were maintained at 37 °C in a humidified incubator with 5% CO_2, and the culture medium was replaced every 3–4 days. The cells were subcultured at approximately 80–90%confluence using 0.25% trypsin–EDTA. After trypsinization, cells were processed by centrifugation to remove floating debris, and only viable cells were used for subsequent experiments.

Reagent preparation and treatment

NaB (Sigma-Aldrich, St. Louis, MO, USA) was dissolved in ultrapure water (UPW) to prepare a sterile 5 M stock solution and diluted in culture medium immediately before use. Cells were treated with NaB at the indicated concentrations for the specified time periods.

CCK-8 assay

Cell viability was assessed using the Cell Counting Kit-8 (CCK-8)(Abcam, Cambridge, UK) according to the manufacturer's instructions. Cells were seeded into 96-well plates and allowed to adhere overnight. Following the indicated treatments, CCK-8 solution was added to each well and the plates were incubated at 37 ℃, 5% CO_2 for 2–3 h. Absorbance was measured at 460 nm using a microplate reader. Cell viability was expressed as a percentage relative to the untreated control.

Cell aggregation assay

Cell aggregation was evaluated using the hanging drop method. Cell suspensions were prepared at a density of 20,000 cells per 25 μL drop and carefully pipetted onto the inner surface of a sterile culture dish lid. The lid was then inverted and placed over the bottom chamber containing phosphate-buffered saline (PBS) to maintain humidity. The cells were incubated at 37 ℃ in a humidified atmosphere with 5% CO_2 for 3 days. Aggregation was monitored and images were captured at the indicated time points using an inverted microscope equipped with a 40x objective lens.

Scratch assay

Cell migration was evaluated using a scratch assay. Cells were seeded into culture plates and grown to approximately 90% confluence. A linear scratch was generated across the cell monolayer using a sterile pipette tip. Detached cells and debris were gently removed by washing with PBS, and fresh culture medium with the indicated treatments was added. Images of the scratched area were captured at 0 h and at the indicated time points using an inverted microscope equipped with a 40x objective lens.

Western blot

Protein expression was analyzed by western blotting. Cells were lysed using radioimmunoprecipitation assay (RIPA) buffer supplemented with a protease inhibitor cocktail. Cell lysates were clarified by centrifugation, and protein concentrations were determined using Bradford assay with bovine serum albumin (BSA) as a standard. Equal amounts of protein were separated by sodium dodecyl sulfate-polyacrylamide gel electrophoresis (SDS-PAGE) and transferred onto membranes. Membranes were blocked with 2% BSA in Tris-buffered saline containing 0.1% Tween-20 (TBS-T), and then incubated with specific primary antibodies overnight at 4 ℃. After washing with TBS-T, the membranes were treated with horseradish peroxidase (HRP)-conjugated secondary antibodies for 1 h. Protein bands were visualized using an KwikQuant Ultra Digital-ECL Substrate solution and KwikQuant Pro Imager (Kindle Biosciences, Greenwich, CT, USA).

Annexin V & PI staining

Apoptosis was assessed using Annexin V and propidium iodide (PI) staining. Cells were harvested after the indicated treatments, washed with cold PBS, and resuspended in Annexin binding buffer. Annexin V and PI were added according to the manufacturer's instructions, and the cells were incubated for 15 min at room temperature in the dark. Following incubation, fluorescence signals of samples were analyzed using a flow cytometer (LSRFortessa™, BD Biosciences, USA). The proportions of viable (Annexin V^-/PI^-), early apoptotic (Annexin V^+/PI^-), and late apoptotic or necrotic (Annexin V^+/PI^+) cells were quantified.

Assessment of MMP

MMP was evaluated using tetramethylrhodamine ethyl ester (TMRE). Carbonyl cyanide 4-(trifluoromethoxy) phenylhydrazone (FCCP) was used as a positive control to induce mitochondrial depolarization. After the indicated treatments, one control group was incubated with FCCP (20 μM) for 10 min at 37 °C in the dark. Cells were

subsequently stained with TMRE (100 nM) for 30 min at 37 °C in the dark, followed by washing with PBS.

For flow cytometry analysis, TMRE-stained cells were analyzed using a flow cytometer (LSRFortessa™, BD Biosciences, USA), and MMP levels were quantified based on TMRE fluorescence intensity. For confocal microscopy, TMRE-stained cells were observed using a laser scanning confocal microscope (Zeiss LSM880 Airyscan, Carl Zeiss, Germany). Changes in MMP were visualized based on TMRE fluorescence, and representative images were acquired using a 561 nm excitation laser, and fluorescence emission was collected in the appropriate TMRE detection range.

Cell cycle assay

Cell cycle distribution was analyzed by flow cytometry using PI staining. Cells were cultured to approximately 60–70% confluence and subjected to the indicated treatments. Following treatment, both adherent and floating cells were collected, washed with PBS, and resuspended in staining buffer. Cells were incubated with RNase A and PI for 30 min to 2 h at room temperature in the dark. After staining, samples were analyzed using a flow cytometer (LSRFortessa™, BD Biosciences, USA), and the proportions of cells in the G0/G1, S, and G2/M phases were quantified based on DNA content.

Quantitative polymerase chain reaction (qPCR)

Total RNA was isolated from cells using the AccuPrep® Universal RNA Extraction Kit (Bioneer) according to the manufacturer's instructions. The extracted RNA was reverse-transcribed into complementary DNA (cDNA) using AccuPower® RT PreMix (Bioneer). Quantitative polymerase chain reaction (qPCR) was performed using gene-specific primer pairs targeting TYMS, TK1, RRM2, DPYD, DHODH, CCNA2, CCNB1, CCND1, CCNE1 and others. Amplification reactions were carried out using AccuPower® 2x GreenStar™ qPCR Master Mix (Bioneer) following the manufacturer's protocol. Relative gene expression levels were calculated using the 2^{-} ΔΔCt method and normalized to GAPDH as an internal control.

Statistical analysis

All experiments were performed in three independent replicates. Statistical analyses were conducted using LSMEANS with Tukey's post hoc test (SAS 9.4), and a p-value < 0.05 was considered statistically significant.

Results

NaB inhibits cell viability and migration in EC cells

To investigate the anti-cancer effects of NaB on EC cells, we first examined its impact on cell viability using HEC1A and AN3CA cell lines. NaB resulted in a dose-dependent decrease in cell viability in both cell lines (Fig. 1A). Notably, HEC1A cells exhibited significantly greater sensitivity to NaB compared to AN3CA cells. We next evaluated the effect of NaB on cell aggregation and migration. NaB suppressed cell aggregation in a dose-dependent manner in both EC cells (Fig. 1B). While baseline aggregation capacity differed between the two cell lines, with AN3CA cells forming compact aggregates and HEC1A cells showing limited aggregation [33–35], both cell lines exhibited clear dose-dependent inhibition of aggregation upon NaB treatment. NaB also suppressed cell migration in a dose-dependent manner in both cell lines (Fig. 1C). HEC1A cells demonstrated a greater reduction in migratory capacity compared to AN3CA cells, suggesting differential sensitivity between these two EC subtypes.

To elucidate the molecular mechanisms underlying the differential anti-migratory effects of NaB, we examined the expression of EMT-related markers. E-cadherin, an epithelial marker crucial for cell-cell adhesion, and mesenchymal markers N-cadherin and Vimentin were analyzed following NaB treatment. In HEC1A cells, NaB treatment induced a dose-dependent increase in E-cadherin expression, while N-cadherin levels decreased accordingly. Vimentin expression remained relatively unchanged. In contrast, AN3CA cells, an endometrial epithelial cancer cell line known to lack E-cadherin expression [36], showed no detectable E-cadherin after NaB treatment. N-cadherin expression decreased in a dose-dependent manner, while Vimentin levels remained largely unaffected, similar to the pattern observed in HEC1A cells (Fig. 1D). These results demonstrate that NaB inhibits cell viability, 3D growth, and migration in EC cells, with differential sensitivity between HEC1A and AN3CA cells, accompanied by modulation of EMT-related markers. To evaluate whether these effects were attributable to physicochemical changes in the culture conditions, we measured the pH of cell-free growth medium following NaB treatment. The pH remained within the physiological range across all tested concentrations and time points and did not differ significantly from untreated controls (Figure S1). In addition, NaB did not reduce the viability of normal endometrial cells even at concentrations that markedly suppressed EC cell growth (Figure S2).

NaB enhances apoptosis in HEC1A cells but not in AN3CA cells

To determine whether the anti-proliferative effects of NaB were associated with apoptosis, we assessed apoptotic cell populations following NaB treatment. HEC1A cells showed a significant dose-dependent increase in apoptotic cell population (yellow-boxed region), with percentages rising from 1.7% to 20.8%. In contrast, AN3CA

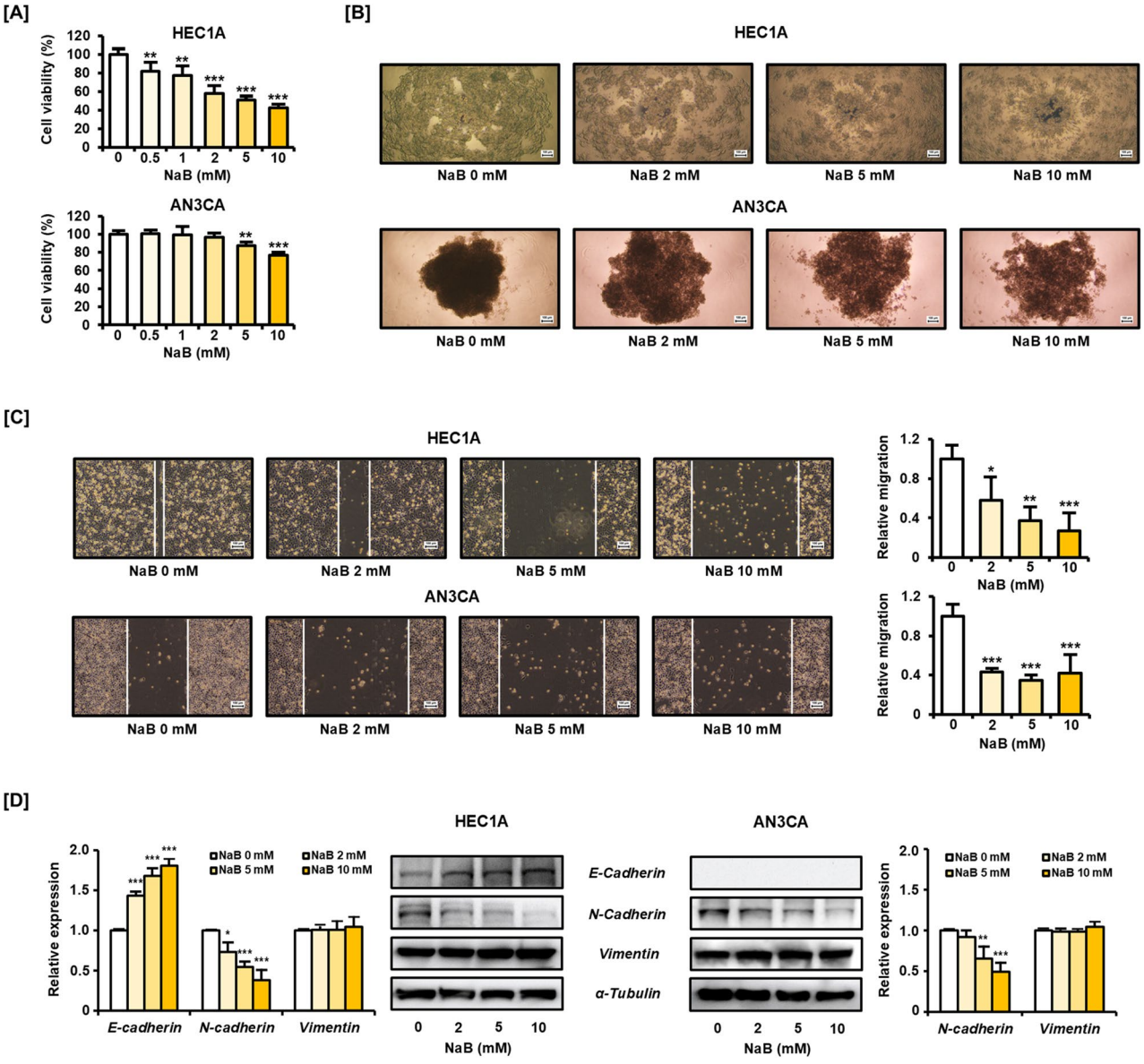


Fig. 1 Effects of NaB on cell viability, spheroid formation, migration, and EMT markers in EC cells. (**A**) Cell viability of HEC1A and AN3CA cells treated with NaB (0, 0.5, 1, 2, 5, and 10 mM) for 48 h, analyzed by CCK-8 assay. (**B**) Cell aggregation in HEC1A and AN3CA cells treated with NaB (0, 2, 5, and 10 mM) for 3 days. Representative images at 3 days (Scale bars = 100 μm) are shown. AN3CA cells formed compact cell aggregates, whereas HEC1A cells demonstrated limited aggregation capacity, consistent with reported cell line-specific variations. (**C**) Cell migration of HEC1A and AN3CA cells treated with NaB (0, 2, 5, and 10 mM), analyzed by scratch assay. Representative images at 24 h (Scale bars = 100 μm) and quantification of relative migration are shown. (**D**) EMT markers in HEC1A and AN3CA cells treated with NaB (0, 2, 5, and 10 mM) for 24 h, analyzed by Western blot. α-Tubulin was used as a loading control. Data are presented as mean values, and error bars indicate SD ($n = 3$). Statistical significance is indicated by asterisks (*$p < 0.05$, **$p < 0.01$, and ***$p < 0.001$ vs. control)

cells exhibited only a modest increase with percentages rising from 1.9% to 4.6%, which was not statistically significant compared to the untreated control (Fig. 2A). To further confirm the apoptotic response at the molecular level, we examined the expression of poly (ADP-ribose) polymerase (PARP), a well-established apoptosis marker, following NaB treatment. In HEC1A cells, NaB induced a dose-dependent increase in cleaved PARP expression relative to full-length PARP, consistent with the robust enhancement of apoptotic pathways. However, AN3CA cells showed no detectable cleaved PARP expression at any NaB concentration tested, with only full-length PARP being observed (Fig. 2B). These results indicate that NaB markedly enhances apoptosis in HEC1A cells in a dose-dependent manner, whereas AN3CA cells may exhibit resistance to NaB-induced apoptosis.

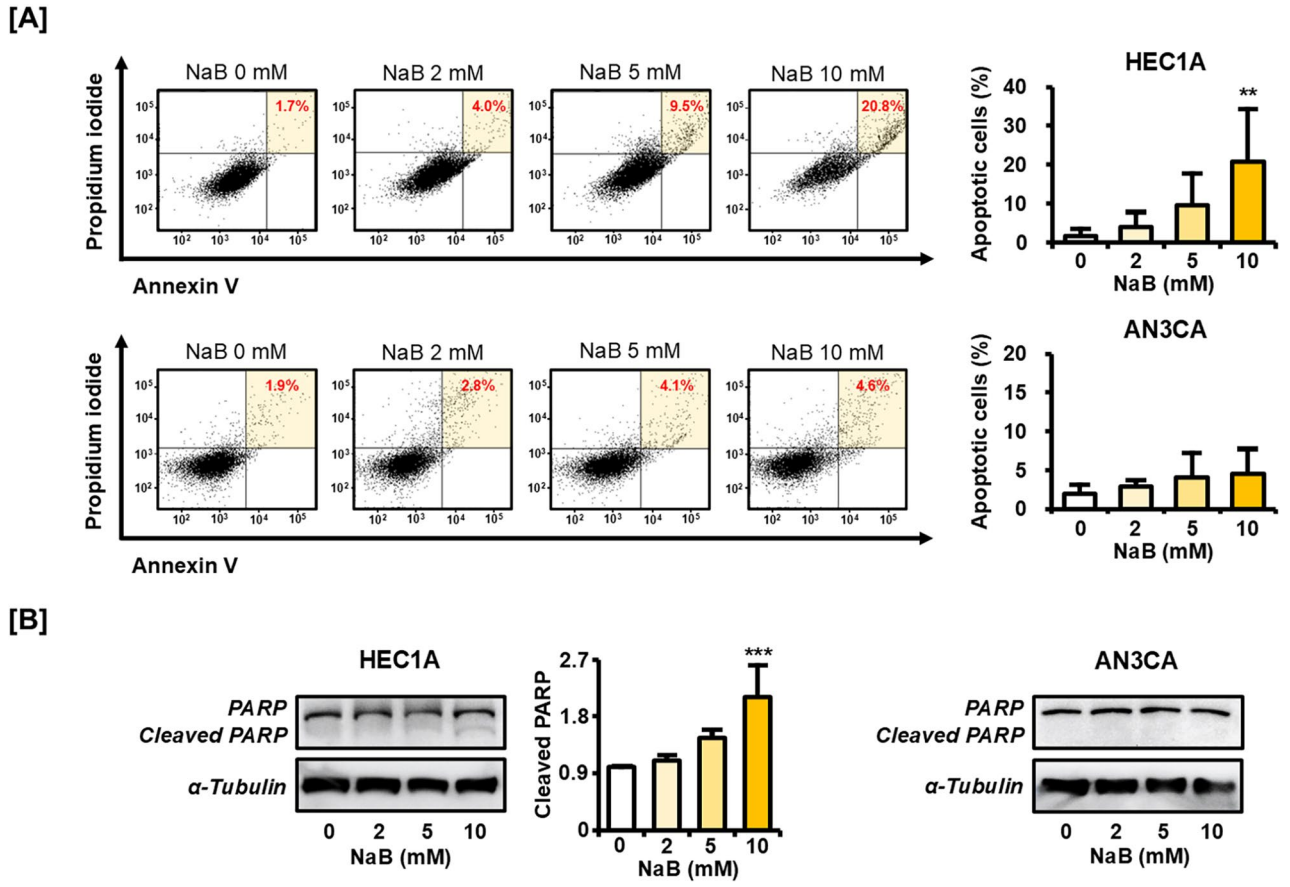


Fig. 2 Effects of NaB on apoptosis in EC cells. (**A**) Apoptotic cells in HEC1A and AN3CA cells treated with NaB (0, 2, 5, and 10 mM) for 48 h, analyzed by Annexin V/PI staining and flow cytometry. Representative dot plots (left) and quantification of apoptotic cell populations (right) are shown. The percentage of apoptotic cells is indicated in the upper right quadrant. (**B**) PARP cleavage in HEC1A and AN3CA cells treated with NaB (0, 2, 5, and 10 mM) for 24 h, analyzed by Western blot. α-Tubulin was used as a loading control. Data are presented as mean values, and error bars indicate SD ($n = 3$). Statistical significance is indicated by asterisks (*$p < 0.05$, **$p < 0.01$, and ***$p < 0.001$ vs. control)

NaB disrupts mitochondrial membrane potential in EC cells

Given the distinct apoptotic responses observed between HEC1A and AN3CA cells, we investigated whether NaB affects mitochondrial membrane potential (MMP), a critical indicator of mitochondrial function and early apoptotic events. NaB treatment (10 mM) clearly reduced MMP in both cell lines. In HEC1A cells, MMP decreased to 30.4% of the control level, while in AN3CA cells, it was reduced to 10.5%, comparable to the effect of FCCP, a mitochondrial uncoupler (Fig. 3A). To further examine the dose-dependent effects of NaB on mitochondrial function, we quantified cells with low MMP following treatment with NaB (0, 2, 5 and 10 mM). The percentage of cells with depolarized mitochondria increased dose-dependently in both cell lines. In HEC1A cells, the low MMP population increased from 11.7% to 34.4% as NaB concentration increased, while AN3CA cells showed a more pronounced response, rising dramatically from 3.4% to 44.1% (Fig. 3B). These results demonstrate that NaB induces mitochondrial membrane depolarization in EC cells in a dose-dependent manner, indicating disruption of mitochondrial function.

NaB induces cell cycle arrest with distinct patterns in EC cells

To investigate the mechanism underlying the anti-proliferative effects of NaB, we examined its impact on cell cycle distribution following treatment with NaB (0, 2, 5 and 10 mM). In HEC1A cells, NaB induced a marked dose-dependent increase in subG1 population, accompanied by decreases in G1, S, and G2/M phases. In contrast, AN3CA cells showed a moderate increase in subG1 with concurrent G1 accumulation and G2/M reduction, while the S phase remained relatively unchanged. The pronounced subG1 accumulation in HEC1A cells is consistent with the extensive apoptosis observed in this cell line, whereas G1 accumulation in AN3CA cells suggests cell cycle arrest (Fig. 4A). To elucidate the molecular mechanisms underlying these differential responses, we examined the mRNA expression of key cell cycle regulators following NaB treatment (10 mM). In HEC1A

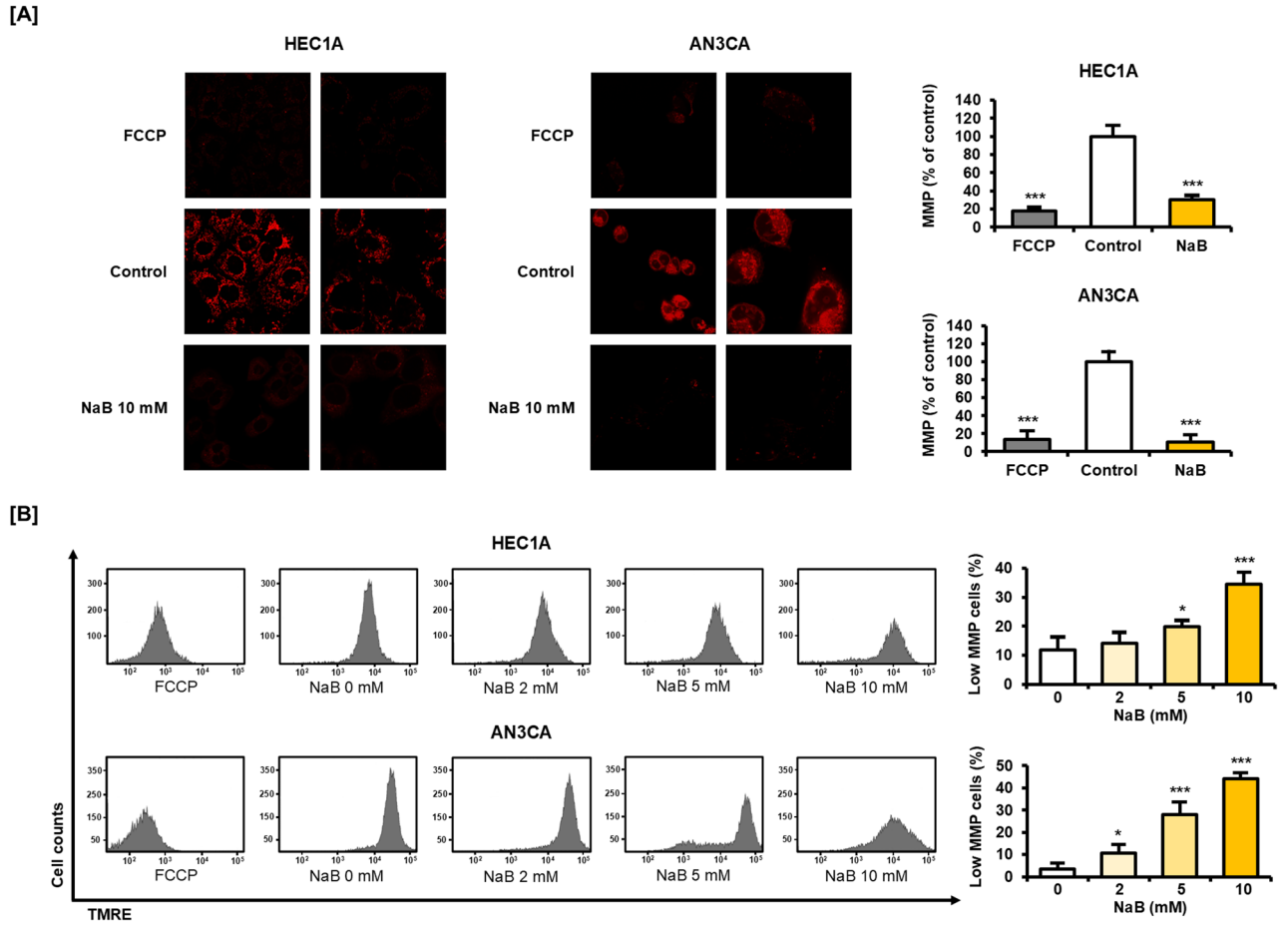


Fig. 3 Effects of NaB on MMP in EC cells. (**A**) MMP in HEC1A and AN3CA cells treated with NaB (0, 2, 5, and 10 mM) for 24 h, visualized by TMRE staining and confocal microscopy. FCCP (20 μM) was used as a positive control. Representative images (left) and quantification of MMP (right) are shown. (**B**) Low MMP cell populations in HEC1A and AN3CA cells treated with NaB (0, 2, 5, and 10 mM) for 24 h, analyzed by TMRE staining and flow cytometry. FCCP (20 μM) was used as a positive control. Representative histograms (left) and quantification (right) are shown. Data are presented as mean values, and error bars indicate SD ($n = 3$). Statistical significance is indicated by asterisks (*$p < 0.05$, **$p < 0.01$, and ***$p < 0.001$ vs. control)

cells, NaB downregulated transcription factors c-Myc, FOXM1, and E2F1, as well as cyclins (CCNB1, CCNA2, CCNE1, CCND1) and cyclin-dependent kinase CDK2. In AN3CA cells, c-Myc, FOXM1, CCNB1, and CCNA2 were downregulated, whereas E2F1, CDK2, CCNE1, and CCND1 were upregulated (Fig. 4B). These results indicate that NaB disrupts cell cycle progression through distinct mechanisms in the two cell lines, with HEC1A cells undergoing extensive apoptosis and AN3CA cells experiencing G1 phase arrest.

NaB modulates pyrimidine metabolism enzymes in EC cells

Given the observed effects of NaB on cell growth and cell cycle progression, and the essential role of pyrimidine metabolism in supporting nucleotide supply for proliferating cells, we next examined key enzymes involved in pyrimidine metabolism at the protein level. NaB treatment (0, 2, 5, and 10 mM) resulted in a dose-dependent decrease in TS expression, while thymidine kinase 1 (TK1) showed the opposite pattern with increased expression in both HEC1A and AN3CA cells. In contrast, RRM2, DHFR, and DTYMK remained relatively unchanged in both cell lines (Fig. 5A). To further examine the effects of NaB on pyrimidine metabolism, we analyzed the mRNA expression of enzymes involved in de novo pyrimidine synthesis, salvage pathways, and related metabolic processes following NaB treatment (10 mM). Among enzymes supporting nucleotide biosynthesis, DHFR and RRM2 were downregulated in HEC1A, but increased in AN3CA. MTHFR showed opposite patterns between the two cell lines, with increase in HEC1A and decrease in AN3CA (Fig. 5B). In de novo synthesis pathway, TYMS, encoding TS, was significantly downregulated in both cell lines, consistent with protein-level observations. Other key enzymes (CAD, DHODH, UMPS) were also decreased in HEC1A, with UMPS showing particularly strong suppression. In AN3CA, CAD and UMPS were decreased, while DHODH was

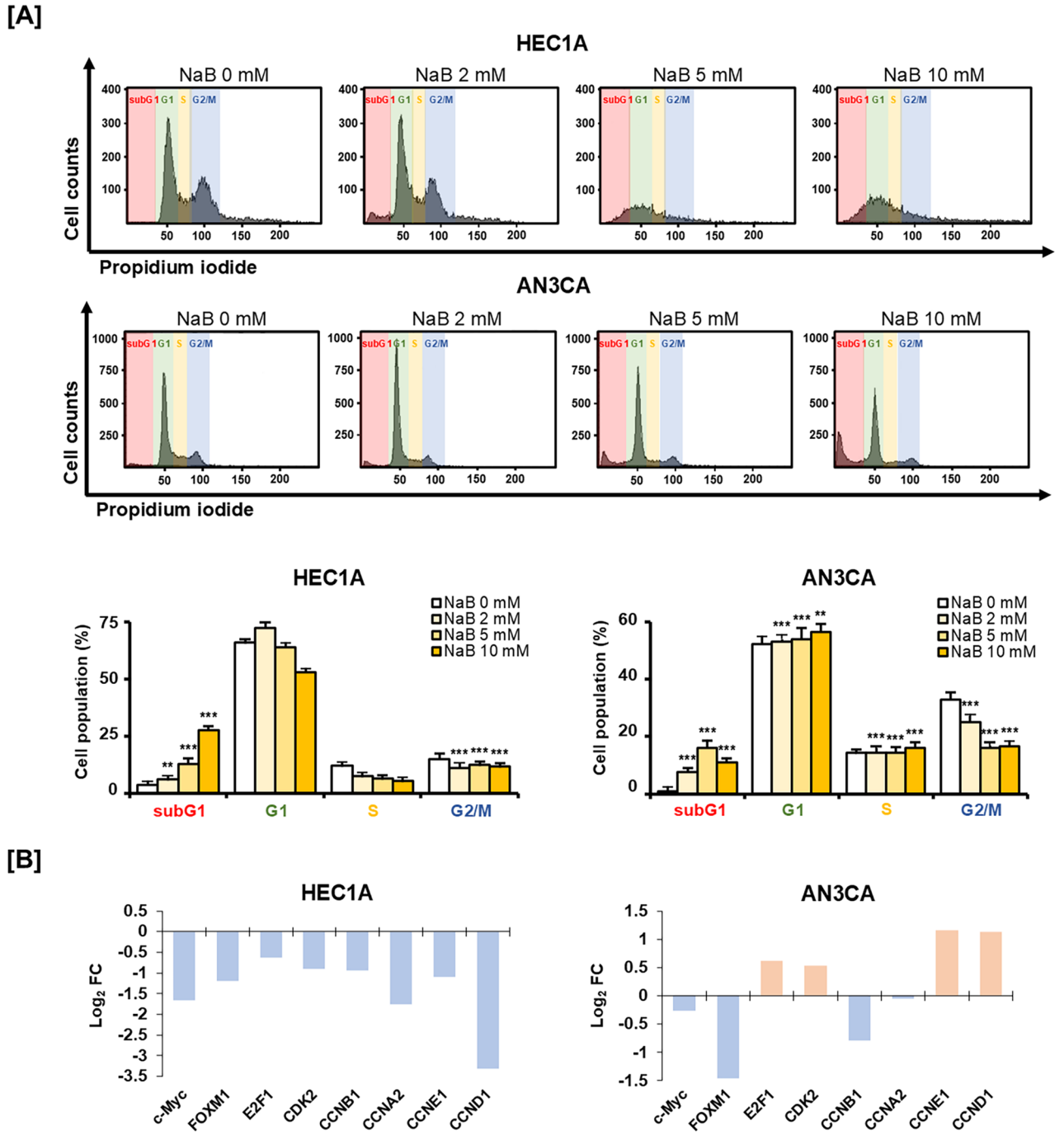


Fig. 4 Effects of NaB on cell cycle progression in EC cells. (**A**) Cell cycle distribution of HEC1A and AN3CA cells treated with NaB (0, 2, 5, and 10 mM) for 24 h, analyzed by PI staining and flow cytometry. Representative histogram (top) and quantification of cell populations in each phase (bottom) are shown. (**B**) Relative mRNA expression of cell cycle-related genes in HEC1A and AN3CA cells treated with NaB (10 mM) for 24 h, analyzed by qPCR. Data are presented as log2 fold change compared to control. Data are presented as mean values, and error bars indicate SD ($n = 3$). Statistical significance is indicated by asterisks (*$p < 0.05$, **$p < 0.01$, and ***$p < 0.001$ vs. control)

increased. In the salvage pathway, UCK2 and UPP1 showed variable responses between cell lines, whereas TK1 and TYMP were consistently upregulated in both cell lines. Pyrimidine degradation enzymes DPYS and UPB1 were decreased in both cell lines. Taken together, these results indicate that NaB induces broad alterations in pyrimidine metabolism in EC cells. In particular, the consistent suppression of TS, a key enzyme in de novo thymidylate synthesis, together with the upregulation of salvage pathway-related genes, suggests that NaB is

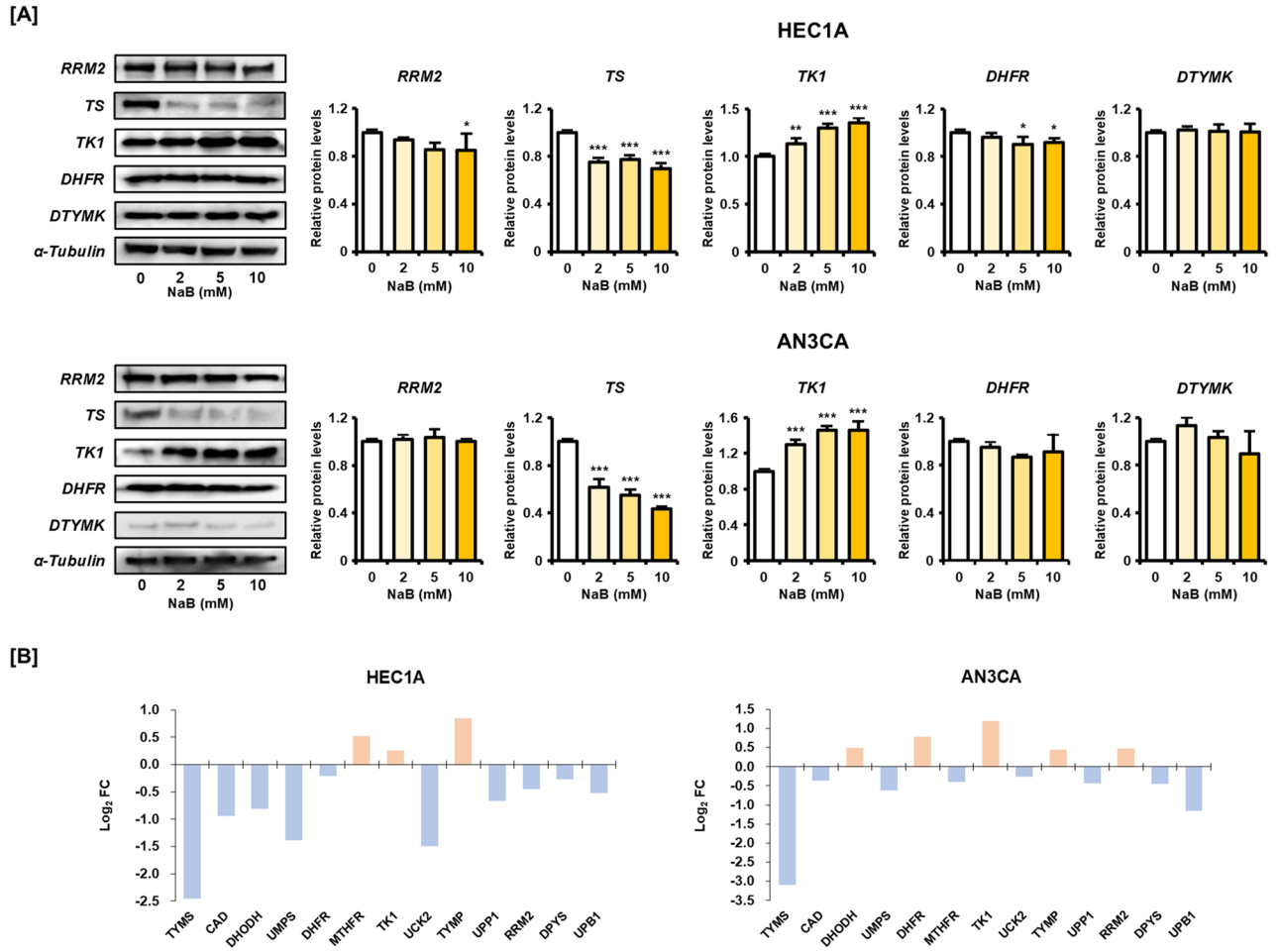


Fig. 5 Effects of NaB on pyrimidine metabolism-related enzymes in EC cells. (**A**) Protein expression of pyrimidine metabolism enzymes (RRM2, TS, TK1, DHFR, DTYMK) in HEC1A and AN3CA cells treated with NaB (0, 2, 5, and 10 mM) for 24 h, analyzed by Western blot. α-Tubulin was used as a loading control. Representative blots (left) and quantification (right) are shown. (**B**) Relative mRNA expression of pyrimidine metabolism-related genes in HEC1A and AN3CA cells treated with NaB (10 mM) for 24 h, analyzed by qPCR. Data are presented as log2 fold change compared to control. Data are presented as mean values, and error bars indicate SD ($n = 3$). Statistical significance is indicated by asterisks (*$p < 0.05$, **$p < 0.01$, and ***$p < 0.001$ vs. control)

associated with extensive remodeling of pyrimidine metabolic pathways.

Discussion

In this study, we demonstrated that NaB exerts broad anticancer effects in HEC1A and AN3CA EC cells, by inhibiting cell viability, aggregation, and migration, and by modulating apoptosis, mitochondrial function, cell cycle progression, and pyrimidine metabolism. HEC1A cells were more sensitive to NaB than AN3CA cells, underscoring intrinsic heterogeneity among EC subtypes and extending previous reports of NaB-mediated antiproliferative and anti-migratory effects to EC [13, 30]. NaB markedly enhanced apoptosis in HEC1A but not AN3CA cells, despite inducing mitochondrial membrane depolarization in both lines. This discordance suggests that AN3CA cells may harbor compensatory survival mechanisms that uncouple mitochondrial damage from apoptotic execution, potentially involving death receptor signaling, autophagy, or non-apoptotic pathways such as ferroptosis. Indeed, recent work has shown that NaB can induce ferroptosis in EC via the RBM3/SLC7A11 axis [37], supporting the notion that NaB triggers distinct cell death programs depending on cellular context. Cell cycle analyses further revealed cell line-specific responses: dramatic subG1 accumulation in HEC1A versus G1 arrest with limited apoptosis in AN3CA. The paradoxical upregulation of E2F1, CDK2, CCNE1, and CCND1 in AN3CA despite downregulation of c-Myc, FOXM1, CCNB1, and CCNA2 in both cell lines suggests a compensatory transcriptional program supporting survival and cell cycle re-entry, consistent with previous reports of NaB-induced arrest and senescence in gynecologic cancers [38]. Taken together, these findings suggest that although the downstream responses to NaB differ

between EC cell lines, its overall growth-inhibitory effect is preserved across distinct cellular contexts.

The most novel finding of our study is the potent and consistent suppression of thymidylate synthase (TS/TYMS) by NaB at both mRNA and protein levels in EC cells. To our knowledge, direct evidence linking NaB to TS suppression remains scarce, with only limited reports in colorectal and gastric cancer [13, 30], and no prior study has demonstrated this mechanism in EC. This is of considerable significance, as TS is a key enzyme in de novo thymidylate synthesis and the primary target of 5-fluorouracil (5-FU). TS inhibition disrupts S-phase progression, induces replication stress, and activates DNA damage checkpoints. Thus, our focus on TS and pyrimidine metabolism was guided by the consistent suppression of TS observed in our experimental data, as well as the central role of this pathway in supporting DNA synthesis and proliferative demand in cancer cells. In addition, previous studies have suggested that pyrimidine metabolism has biological and clinical relevance in EC, further supporting the rationale for examining this pathway in the present study. By identifying TS suppression as a prominent molecular event associated with NaB treatment in EC, our findings support further preclinical investigation of whether modulation of this pathway may influence fluoropyrimidine response in EC models. Beyond TS, NaB broadly reprogrammed pyrimidine metabolism by downregulating de novo pathway enzymes including CAD and UMPS, while differentially regulating DHODH and folate-related genes such as DHFR and MTHFR. Since DHODH is a mitochondria-dependent step in de novo pyrimidine synthesis, NaB-induced mitochondrial depolarization may further exacerbate nucleotide depletion by limiting DHODH activity - mechanistically linking mitochondrial dysfunction to pyrimidine insufficiency. Concurrently, NaB upregulated TK1 and several salvage pathway enzymes, likely as a compensatory response to impaired de novo synthesis. However, this salvage activation appeared insufficient to prevent viability loss, implying that co-targeting salvage enzymes could further intensify nucleotide stress and enhance efficacy.

NaB also modulated EMT-related markers in a cell line-specific manner, increasing E-cadherin and decreasing N-cadherin in HEC1A cells, while reducing N-cadherin without altering vimentin in E-cadherin-deficient AN3CA cells. Both lines showed dose-dependent suppression of migration and aggregation, indicating that NaB inhibits motility regardless of baseline EMT status. Given butyrate's context-dependent effects on EMT reported in other tumor types [39], our data highlight EC as a setting in which NaB predominantly exerts anti-migratory and potentially anti-metastatic effects.

Collectively, these findings provide important mechanistic insight into how NaB affects EC cell metabolism and growth-related pathways. However, the effective concentrations of NaB used in the present in vitro study were in the millimolar range, and such concentrations are unlikely to be readily achievable systemically in humans under physiological or standard therapeutic conditions. Therefore, the present findings should not be interpreted as direct evidence supporting NaB as a systemic therapeutic agent for EC. Rather, our results are more appropriately viewed as demonstrating the mechanistic potential of NaB as a metabolic modulator in EC cells and as providing a rationale for further investigation in settings where local delivery or context-specific exposure may be more feasible. In addition, although immortalized normal endometrial cells showed a response pattern distinct from that of EC cells, additional non-malignant endometrial cell models will be required to define the selectivity of NaB more clearly. Furthermore, the present study was conducted primarily under in vitro conditions, and in vivo studies will be necessary to determine whether the observed metabolic and molecular effects of NaB are recapitulated in a more physiologically relevant tumor environment. The differential responses observed between HEC1A and AN3CA cells nevertheless suggest that cellular context may influence the downstream consequences of NaB exposure, supporting the need for further mechanistic and preclinical studies that consider the molecular and metabolic heterogeneity of EC.

In conclusion, NaB exerts multifaceted growth-suppressive effects in EC cells and is associated with MMP disruption, cell line-specific apoptosis and cell cycle arrest, and reprogramming of pyrimidine metabolism with prominent TS suppression. To our knowledge, this is the first study to demonstrate a strong association between NaB treatment and TS downregulation in EC. These findings provide mechanistic insight into the in vitro metabolic effects of NaB and support further investigation of pyrimidine metabolism-related vulnerabilities in preclinical EC models.

Supplementary Information

The online version contains supplementary material available at https://doi.org/10.1186/s12263-026-00805-z.

Supplementary Material 1

Supplementary Material 2

Author contributions

Conceptualization: Changwon Yang. Data curation: Nayeon Kim. Formal analysis: Nayeon Kim, Sooyeon Park. Funding acquisition: Changwon Yang. Investigation: Nayeon Kim. Methodology: Nayeon Kim, Changwon Yang. Project administration: Nayeon Kim. Supervision: Changwon Yang. Validation: Nayeon Kim. Visualization: Nayeon Kim, Sooyeon Park. Writing – original draft preparation: Nayeon Kim. Writing – review and editing: Sooyeon Park, Changwon Yang. All authors have read and approved the final manuscript.

Funding
This work was supported by the National Research Foundation of Korea(NRF) grant funded by the Korea government(MSIT) (RS-2025-00516653).

Data availability
The data presented in this study are available on request from the corresponding author.

Declarations

Ethics approval
This study involved only in vitro experiments using established cell lines and did not include human participants, human tissues, or animals.

Competing interests
The authors declare no competing interests.

Received: 13 March 2026 / Accepted: 27 April 2026
Published online: 02 May 2026

References

1. Corr BR, et al. Advances in the management of endometrial cancer. BMJ. 2025;388:e080978.
2. Colombo N, et al. ESMO-ESGO-ESTRO consensus conference on endometrial cancer: Diagnosis, treatment and follow-up. Radiother Oncol. 2015;117(3):559–81.
3. Bray F, et al. Global cancer statistics 2018: GLOBOCAN estimates of incidence and mortality worldwide for 36 cancers in 185 countries. CA Cancer J Clin. 2018;68(6):394–424.
4. Lortet-Tieulent J, et al. International Patterns and Trends in Endometrial Cancer Incidence, 1978–2013. J Natl Cancer Inst. 2018;110(4):354–61.
5. Rahib L, et al. Estimated Projection of US Cancer Incidence and Death to 2040. JAMA Netw Open. 2021;4(4):e214708.
6. Bendifallah S, Ilenko A, Daraï E. High risk endometrial cancer: Clues towards a revision of the therapeutic paradigm. J Gynecol Obstet Hum Reprod. 2019;48(10):863–71.
7. Kokka F et al. Hormonal therapy in advanced or recurrent endometrial cancer. Cochrane Database Syst Rev, 2010. 2010(12): p. Cd007926.
8. Tronconi F, et al. Advanced and recurrent endometrial cancer: State of the art and future perspectives. Crit Rev Oncol Hematol. 2022;180:103851.
9. Nong S, et al. Metabolic reprogramming in cancer: Mechanisms and therapeutics. MedComm. 2020;2023(42):pe218.
10. Zhu Y, et al. Metabolic Reprogramming: A Crucial Contributor to Anticancer Drug Resistance. MedComm. 2020;2025(69):pe70358.
11. Li S, et al. Short-chain fatty acids and cancer. Trends Cancer. 2025;11(2):154–68.
12. Son MY, Cho HS. Anticancer Effects of Gut Microbiota-Derived Short-Chain Fatty Acids in Cancers. J Microbiol Biotechnol. 2023;33(7):849–56.
13. Kim N, Yang C. Sodium Butyrate Enhances 5-Fluorouracil sensitivity through thymidylate synthase regulation and cell-cycle modulation in gastric cancer. Mol Nutr Food Res. 2025;69(19):e70152.
14. Li X, et al. Intratumor microbiome-derived butyrate enhances progesterone sensitivity by inducing ferroptosis in endometrial cancer. Pharmacol Res. 2025;219:107902.
15. Tao M, et al. Butyrate enhances gut dysbiosis by activating the cAMP/PKA/CREB signaling pathway to inhibit the progression of endometrial carcinoma. BMC Microbiol. 2025;25(1):516.
16. Chen J, et al. De novo nucleotide biosynthetic pathway and cancer. Genes Dis. 2023;10(6):2331–8.
17. Do BT, et al. Nucleotide depletion promotes cell fate transitions by inducing DNA replication stress. Dev Cell. 2024;59(16):2203–e222115.
18. Fu Y, et al. Discovery of the potential biomarkers for early diagnosis of endometrial cancer via integrating metabolomics and transcriptomics. Comput Biol Med. 2024;173:108327.
19. Xu WH, et al. Association of thymidylate synthase gene with endometrial cancer risk in a Chinese population. Cancer Epidemiol Biomarkers Prev. 2009;18(2):579–84.
20. Martínez-Reyes I, et al. TCA Cycle and Mitochondrial Membrane Potential Are Necessary for Diverse Biological Functions. Mol Cell. 2016;61(2):199–209.
21. Khutornenko AA, et al. Pyrimidine biosynthesis links mitochondrial respiration to the p53 pathway. Proc Natl Acad Sci U S A. 2010;107(29):12828–33.
22. Peeters MJW, et al. Mitochondrial-Linked De Novo Pyrimidine Biosynthesis Dictates Human T-Cell Proliferation but Not Expression of Effector Molecules. Front Immunol. 2021;12:718863.
23. Brisudova P, et al. Functional mitochondrial respiration is essential for glioblastoma tumour growth. Oncogene. 2025;44(30):2588–603.
24. Owusu-Akyaw A, et al. The role of mesenchymal-epithelial transition in endometrial function. Hum Reprod Update. 2019;25(1):114–33.
25. Uchida H. Epithelial mesenchymal transition in human menstruation and implantation. Endocr J. 2024;71(8):745–51.
26. Makker A, Goel MM. Tumor progression, metastasis, and modulators of epithelial-mesenchymal transition in endometrioid endometrial carcinoma: an update. Endocr Relat Cancer. 2016;23(2):R85–111.
27. Sciacovelli M, Frezza C. Metabolic reprogramming and epithelial-to-mesenchymal transition in cancer. Febs j. 2017;284(19):3132–44.
28. Hua W, et al. TGFβ-induced metabolic reprogramming during epithelial-to-mesenchymal transition in cancer. Cell Mol Life Sci. 2020;77(11):2103–23.
29. Mrkvicova A, et al. The effect of sodium butyrate and cisplatin on expression of EMT markers. PLoS ONE. 2019;14(1):e0210889.
30. Kim N, Yang C. Sodium Butyrate Inhibits the Expression of Thymidylate Synthase and Induces Cell Death in Colorectal Cancer Cells. Int J Mol Sci, 2024. 25(3).
31. Sillem M, et al. Invasiveness corresponds to differentiation rather than to proteinase secretion in endometrial cancer cell lines. Eur J Gynaecol Oncol. 1999;20(5–6):367–70.
32. Wang Y, et al. Genomic characterization of gene copy-number aberrations in endometrial carcinoma cell lines derived from endometrioid-type endometrial adenocarcinoma. Technol Cancer Res Treat. 2010;9(2):179–89.
33. Schröpfer A, et al. Expression pattern of matrix metalloproteinases in human gynecological cancer cell lines. BMC Cancer. 2010;10(1):553.
34. Cao M, et al. TMT-based quantitative proteomic analysis of spheroid cells of endometrial cancer possessing cancer stem cell properties. Stem Cell Res Ther. 2023;14(1):119.
35. Harduf H, Goldman S, Shalev E. Progesterone receptor A and c-Met mediates spheroids-endometrium attachment. Reproductive Biology Endocrinol. 2009;7(1):14.
36. Rahnama F, et al. Epigenetic Regulation of E-Cadherin Controls Endometrial Receptivity. Endocrinology. 2009;150(3):1466–72.
37. Wang Z, et al. Sodium butyrate induces ferroptosis in endometrial cancer cells via the RBM3/SLC7A11 axis. Apoptosis. 2023;28(7):1168–83.
38. Terao Y, et al. Sodium butyrate induces growth arrest and senescence-like phenotypes in gynecologic cancer cells. Int J Cancer. 2001;94(2):257–67.
39. Zang W, et al. Butyrate promotes oral squamous cell carcinoma cells migration, invasion and epithelial-mesenchymal transition. PeerJ. 2022;10:e12991.

Publisher's note

Springer Nature remains neutral with regard to jurisdictional claims in published maps and institutional affiliations.